Available online at www.sciencedirect.com
SCIENCE DIRECT
Journal of Catalysis 237 (2006) 38–48
JOURNAL OF CATALYSIS
www.elsevier.com/locate/jcat

Study of new catalysts based on vanadium oxide supported on mesoporous silica for the partial oxidation of methane to formaldehyde: Catalytic properties and reaction mechanism

L.D. Nguyen [a], S. Loridant [a,*], H. Launay [a], A. Pigamo [b], J.L. Dubois [b], J.M.M. Millet [a]

[a] *Member of the European CONCORDE Coordination Action, Institut de Recherches sur la Catalyse, CNRS, 2 av. A. Einstein, 69626 Villeurbanne, France*
[b] *Arkema, Centre de Recherches Rhône-Alpes, rue Henri Moissan, BP 63, 69493 Pierre-Bénite cedex, France*

Received 27 June 2005; revised 14 October 2005; accepted 17 October 2005

Available online 18 November 2005

Abstract

Vanadium oxide supported on mesoporous silica has been synthesized by a novel method and the resulting species tested as catalysts for the partial oxidation of methane to formaldehyde at atmospheric pressure. These catalysts appear to be very active and selective toward formaldehyde. Space–time yields superior to those of all known catalysts of the same type have been obtained. Kinetic parameters all tend to show that the same mechanism postulated for supported vanadium catalyst is taking place. The positive effect of water is also seen. The high performance has been attributed to the wide dispersion of vanadium-isolated species, which are known to be very active and selective, and to greatly superior silanol surface content than in other catalysts. The novel preparation method favors the formation of given isolated species that will be the most active and selective.

Keywords: Vanadium oxide; Mesoporous silica; Partial oxidation; Methane; Formaldehyde

1. Introduction

In the coming century, the petrochemical industry will have to move to the direct use of natural gas as feedstock to fulfill the increasing demand in intermediate chemicals and energy. The direct catalytic oxidation of methane to formaldehyde is certainly a potential route to valorize natural gas, but is the most difficult approach. Although some new catalysts have recently been proposed for this reaction [1,2], their efficiency remains too low to sustain any industrial application. Among the promising systems, vanadium oxide supported on silica catalysts are the most efficient for converting methane to formaldehyde [1,3,4], whereas supported molybdenum oxide catalysts used under specific conditions of activation and testing have been reported to be efficient [5–7].

The studies on supported vanadium oxide catalysts have shown that a key parameter to obtain a good selectivity with such catalysts was the dispersion of the active sites [3,4,8–10]. In that respect, high-surface area mesoporous silica has been used as support and has been shown to favor such dispersion and consequently the selectivity toward formaldehyde. The increased selectivity was certainly also due to the lack of limitation of the diffusion of reactants and products into the mesoporous pores. In most studies, first the mesoporous support was synthesized, and then the vanadium sites were created by either conventional impregnation or grafting methods [1,3,4,8–11]. Very few publications described other methods of preparation. One example is the introduction of vanadium cations directly into the templating agent used to prepare the mesoporous compound or a template–ion exchange method [12,13]. Another example is the synthesis of V_2O_5–SiO_2 xerogels by a two-step sol–gel process [14]. But these procedures led to catalysts with comparable catalytic properties, and their characterization pointed to similar active sites. Although several vanadium species were shown to be active and selective, the most efficient ones appeared to be monomeric or mononuclear species.

* Corresponding author.
E-mail address: stephane.loridant@catalyse.cnrs.fr (S. Loridant).

0021-9517/$ – see front matter
doi:10.1016/j.jcat.2005.10.016

Most kinetic studies agreed that formaldehyde was the primary product, with CO and CO_2 formed mainly in consecutive reactions [8,15,16]. Methanol formation was assumed to occur parallel to that of formaldehyde by hydrolysis of intermediate methoxy species [1].

In the present study, a new preparation method of vanadium-containing mesoporous silica compounds was developed. The objectives were to improve the vanadium site isolation and to see whether an anchorage of the vanadium on the mesoporous silica surface different from that obtained by grafting or impregnation may be achieved, generating particular catalytic properties. The synthesized solids were tested for the methane partial oxidation under various conditions. The influences of contact time and addition of water to the gas feed, both crucial parameters for limiting the consecutive degradation of formaldehyde [4], were investigated. The catalytic performances of the different catalysts were studied and compared with the best performances reported in the literature. Finally, several kinetic parameters were determined, and vanadium-active species were characterized with various techniques.

2. Experimental

2.1. Catalyst preparation

A novel preparation method has been developed to synthesize the vanadium oxide supported on mesoporous silica catalysts [17]. This method is based on the co-condensation of monomeric vanadium $VO_2(OH)_2^-$ and $Si(OC_2H_5)_4$ species at $5 < pH < 6$ in a solution containing a template. The Pourbaix diagram of vanadium reports the vanadium speciation in aqueous solutions as a function of pH and potential at 25 °C [18–20].

For a standard preparation, various quantities of NH_4VO_3 were dissolved in 5 mL of water, 2.72 g of cetyltrimethylammonium bromide (C_{16}TMABr) was dissolved in 50 mL of water, and 30.27 g of NH_4Cl (used as a buffer) was dissolved in 90 mL of water. After these three solutions were mixed, the pH value was adjusted to 5–6 before tetraethoxysilicate (TEOS) was added. The molar proportions of precursors were 0.5 for TEOS, 9.2 for NH_4Cl, 0.12 for C_{16}TMABr, y for NH_4VO_3, and 130 for H_2O. After a reflux of the solution for 24 h at 40 °C, the precipitate was filtered and washed with hot water. The template was extracted by washing with ethanol at 80 °C for 2 h. After drying at 100 °C for 12 h, the compound was calcined at 650 °C for 6 h in air flowing at 50 mL min^{-1}.

We have chosen to refer to the different compounds prepared by their y value, corresponding to the molar proportion of NH_4VO_3 used for the preparation. For example, V12 was prepared with $y = 0.012$. Compound without vanadium was also prepared through this route.

Two reference samples were prepared for comparison with the new catalysts. The first sample, labeled V/MCM-A, was prepared following the impregnation method described previously [4] and using a MCM41 support synthesized according to a published method [21], dried at 120 °C overnight, and finally calcined at 550 °C for 5 h. The second sample, labeled V/MCM-B was synthesized by hydrolysis of TEOS in the presence of a vanadium template in an ethanol solution [13]. The vanadium template was prepared by adding 4.73 g of $C_{16}H_{33}(CH_3)_3NaBr$ to an aqueous solution of 0.115 M of NH_4VO_3. The resulting white precipitate was filtered, washed with deionized water to remove the excess template, and finally dried in air at 50 °C. For the preparation of V/MCM-B, 1.07 g of this vanadium salt was dissolved in 40 mL of ethanol at 30 °C and added to another solution of 40 mL of ethanol containing 9.11 g of $C_{16}H_{33}(CH_3)_3NaBr$. Then 24.66 g of TEOS and 10 mL of water were added. The pH was adjusted to 10 by adding tetramethyl ammonium hydroxide. A white precipitate appeared in the solution refluxed for 3 h 30; this was filtered, washed with ethanol, and dried in air. The compound was finally calcined for 6 h at 600 °C in air.

2.2. Catalyst characterization

The vanadium content of the catalysts was quantitatively determined by atomic absorption (AES-ICP). X-ray diffraction (XRD) patterns were collected with a Brüker D5005 diffractometer using the Ni-filtered Cu-K_α radiation ($\lambda = 1.5418$ Å). They were recorded with 0.02° (2θ) steps in the 3–80 angular range with 1 s counting time per step and between 1° and 10° (2θ) with the same step and 10 s counting time per step. Specific surface areas were measured using the BET method by adsorption of liquid nitrogen on the samples after desorption at 350 °C for 3 h under secondary vacuum. Complete adsorption–desorption isotherms have been recorded on the solids pretreated similarly. Their pore size distributions were determined using the BJH method applied to the adsorption curves [22–24].

TPR curves were recorded from room temperature up to 750 °C at a heating rate of 3° min^{-1}. A 1% H_2–Ar gas mixture was used to reduce the catalysts. The amounts of consumed H_2 were determined by gas chromatography using a DELSI NERMAG catharometer. Sample pretreatment was achieved at 400 °C for 3 h in argon.

Raman spectra were recorded with a Raman Dilor-XY spectrometer in air at 550 °C. They were accurate within ca. 3 cm^{-1}. The 514.53 nm exciting line of an argon–krypton laser was focused using a 50× objective. The laser power on the samples was typically 3 mW.

Self-supporting disks (about 10 mg cm^{-2}) were prepared for infrared examination by pressing the synthesized samples at 4 bars, then treating them in a homemade infrared cell under flowing oxygen at various temperatures. Spectra were recorded at room temperature with a Fourier transform Vector 22 (Brüker) spectrometer.

2.3. Oxidation of methane

The oxidation of methane was achieved in a fixed-bed quartz reactor (9 mm i.d.) at atmospheric pressure. Its internal diameter was reduced to 2 mm after the catalytic bed to increase gas velocity and decrease degradation of formaldehyde. The reaction temperature was measured using a Pt–PtRh thermocouple placed into a thermowell located in the center of the catalytic bed. Nitrogen was used as a dilution gas, and neon was used as

an internal standard. The reactants and gas products were analyzed on-line using a Chrompack CP-3800 gas chromatograph equipped with a thermal conductivity detector, a Hayesep T, and Molsieve 5 Å columns.

The reaction temperature varied between 550 and 600 °C. A feedstock composition of 10% Ne/20% N_2/10% O_2/30% CH_4/30% H_2O was used for the isoconversion study, and another one of 40% N_2/13% O_2/38% CH_4/9% H_2O was used to study the influence of contact time. The gas hourly space velocity (GHSV) value varied from 60,000 to 740,000 L kg_{cat}^{-1} h^{-1}. The products formed under these reaction conditions were formaldehyde, CO, methanol, and CO_2. Traces of C_2H_4 and C_2H_6 were observed above 600 °C. The effect of water was studied by varying the water content between 0 and 30 kPa while keeping the oxygen and methane partial pressures constant. Water vapor was synthesized on-line, sending a hydrogen–oxygen mixture on a Pt/Al_2O_3 filled column heated at 210 °C.

Blank tests without catalyst were performed to demonstrate that the homogeneous reaction was negligible up to 600 °C. Carbon balances were systematically calculated and proved satisfactory for all of the runs to within ±2%. Chemical analyses of formaldehyde were performed as described previously [5] to confirm the results obtained by gas chromatography (GC). For that purpose, a straight quartz reactor was used, and formaldehyde was trapped in water cooled with ice by bubbling in an aqueous solution containing an excess of Na_2SO_3 and a defined quantity of H_2SO_4. The remaining gas (CH_4, CO, and CO_2) was analyzed by GC as described above. This allowed to indirectly measure HCHO that reacted with Na_2SO_3 to produce NaOH, which immediately consumed H_2SO_4. The remaining quantity of H_2SO_4 was finally titrated by a standard solution of NaOH using phenolphthalein. The initial quantity was determined in the same way after equilibrium between Na_2SO_3 and H_2SO_4.

3. Results

3.1. Characterization of the catalysts

The physicochemical characteristics of the prepared catalysts are presented in Table 1. The measured vanadium compositions fitted relatively well with those chosen for the synthesis, and the silicon synthesis yields were systematically >90%. All of the values of the specific surface areas of the solids were around 1000 m^2 g^{-1}, except that of the compound without vanadium, which was slightly higher. These values are typical of those for mesoporous materials [25,26]. No significant decrease in specific surface area was observed with an increase in vanadium content, in contrast to the impregnated V/MCM-41 and V/SBA compounds [3,4,15,20]. The shape of the adsorption–desorption isotherms confirmed that the compounds were mesoporous. The average pore size deduced from the isotherms using the BJH method [22] was typically 3 nm (Table 1).

The powder XRD patterns of the solids (Fig. 1) showed only a broad peak at around $2\theta = 1.7$–$2.0°$ ($d = 4.4$–5.2 nm) assigned to the (100) reflection. These values are typical of poorly ordered mesoporous materials [21]; when the vanadium content increased, the intensity of the peak decreased while its width increased. This demonstrated that adding vanadium had a negative effect on crystallinity. Finally, no peak corresponding to V_2O_5 was detected in the XRD patterns in the 3–80° (2θ) range.

Table 1
Comparison of theoretical and experimental vanadium content (determined by chemical analysis using AES-ICP), specific surface areas and average pore sizes of the prepared V/SiO_2 catalysts

Catalyst	V content (wt%)		SSA (m^2/g)	Pore size (nm)
	Theoretical	Experimental		
Support	–	–	1140	–
V08	1.3	1.3	1020	–
V12	2.2	1.9	990	3.1
V16	2.6	2.5	1010	3.2
V20	3.2	3.0	990	3.3
V24	3.8	3.5	1010	–
V/MCM-A	–	2.8	680[a]	3.0[a]
V/MCM-B	3.3	3.5	620	<4.0

[a] Values reported in Ref. [4].

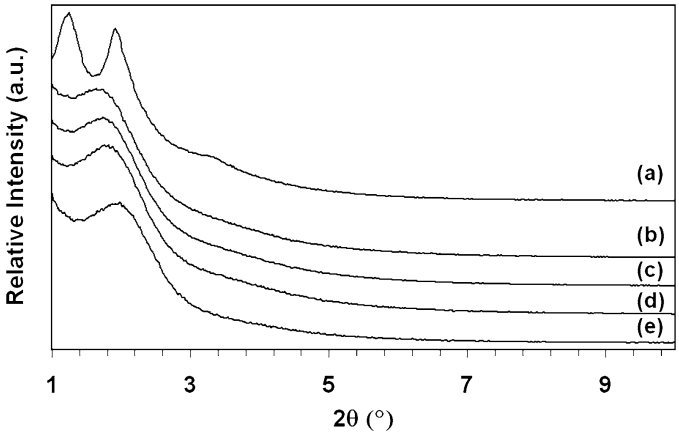

Fig. 1. XRD diagrams of: (a) the mesoporous support, (b) V08, (c) V12, (d) V16 and (e) V20.

3.2. Catalytic properties

A good stability in the yield in formaldehyde was observed for all of the catalysts tested, although the conversion decreased slightly with time on stream for the first 40 h. The slight decrease in specific surface area measured after test could explain this evolution. Consequently, the values of catalytic performance reported in the tables and figures that follow were obtained after stabilization.

Catalysts with various vanadium loadings (V08–V20) were tested between 550 and 600 °C with the same gas feedstock (10% Ne/20% N_2/10% O_2/30% CH_4/30% H_2O) and flow rate but with various catalytic masses to maintain the same conversion on all of the solids. The results obtained at 1.1 and 10.4% of conversion are plotted in Fig. 2. The main reaction products on all of the catalysts were formaldehyde and CO. At 550 °C and 1.1% of conversion, the selectivities in HCHO were >80% (Fig. 2A), and small amounts of CO_2 and methanol

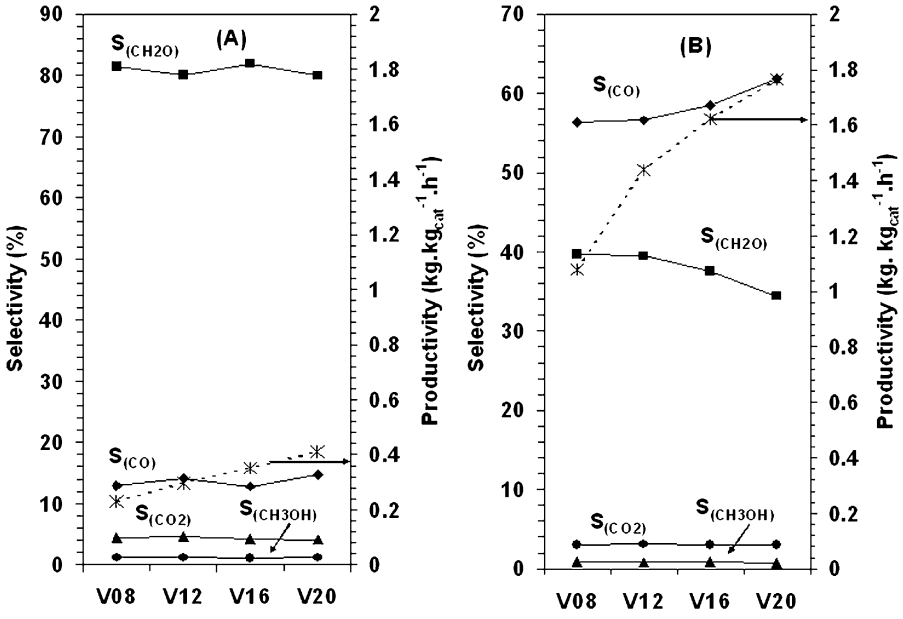

Fig. 2. Catalytic performances of the V08–V20 catalysts at: (A) 1.1% of conversion ($T = 550\,^{\circ}C$) and (B) 10.4% of conversion ($T = 600\,^{\circ}C$). Feed: 10% Ne/20% N_2/10% O_2/30% CH_4/30% H_2O.

were formed. With increasing vanadium loading, the selectivity in formaldehyde remained almost constant except at high loading, where a decrease was observed. This decrease was amplified at high temperature (Fig. 2B). Nonselective species were presumably activated in this later case. In addition, the selectivity in CO was increased. The productivity in HCHO increased with increasing vanadium content and at temperature of at least 600 °C.

Temperature had a similar effect on the catalytic properties of the various new catalysts. This effect on the V12 catalyst is shown in Fig. 3. Selectivity toward formaldehyde and methanol decreased with temperature, mainly to the benefit of CO. CO_2 formation increased slowly up to 580 °C and then more rapidly above this temperature. This evolution could be due to a consecutive reaction of CO or to a gas-phase reaction of CH_4 above 580 °C.

The influence of contact time on the performance of the V12 catalyst was investigated near 550, 580, and 600 °C (Table 2). The significantly decreased conversion arising from the increased flow rate was not counterbalanced by increased selectivity, especially at low temperatures. Consequently, the HCHO yields decreased with increasing GHSV. However, much better productivities were obtained. The best value measured at 600 °C was 6458 $g\,kg_{cat}^{-1}\,h^{-1}$. Interestingly, the selectivity in CH_3OH increased with increasing GHSV values.

The new catalysts were compared with the reference catalysts presenting comparable vanadium content and prepared by impregnation (V/MCM-A) and with the cetyltrimethylammonium vanadium precursor (V/MCM-B). The new catalysts appeared more productive than the reference catalysts tested at the same GHSV (Table 3). This higher productivity was obtained at a lower temperature and, more importantly, was related to a much higher selectivity toward formaldehyde.

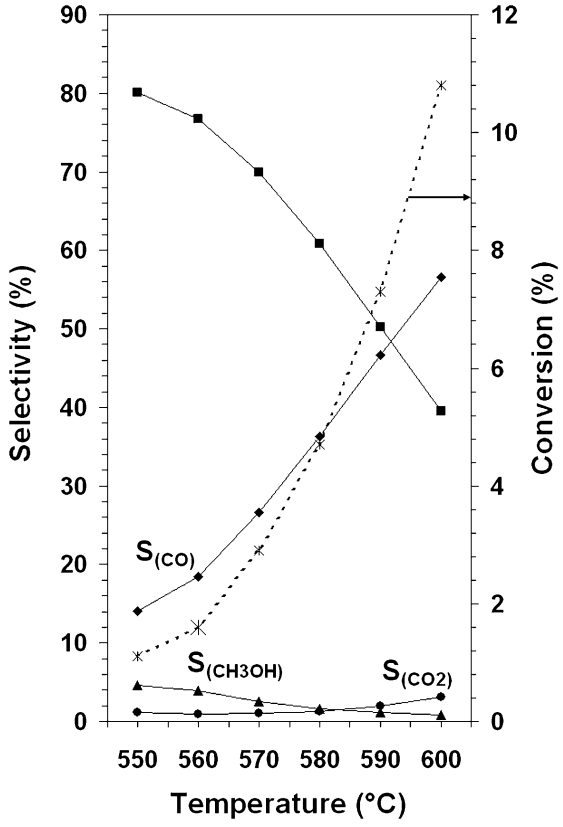

Fig. 3. Influence of temperature on catalytic performances of the V12 catalyst. Feed: 10% Ne/20% N_2/10% O_2/30% CH_4/30% H_2O.

A literature review led us to conclude that the new catalysts were much more productive than any of the catalysts of the same type tested so far (Table 4). Our catalysts differed from the others mainly in terms of their high selectivity at lower re-

Table 2
Influence of contact time on the catalytic performance of the V12 catalyst at 550, 585, and 600 °C

GHSV ($L\,kg_{cat}^{-1}\,h^{-1}$)	T (°C)	Conversion (%)	Selectivity (%)				HCHO productivity ($g\,kg_{cat}^{-1}\,h^{-1}$)
			HCHO	CO	CO_2	CH_3OH	
80,000	552	2.3	82.2	14.9	0.9	2.0	801
	585	7.7	48.9	48.2	2.2	0.7	1548
185,000	549	0.9	91.9	1.4	0.7	6.0	807
	581	3.5	74.2	23.1	1.0	1.8	2435
	600	6.3	57.5	39.9	1.4	1.1	3377
545,000	552	0.2	86.1	0.0	3.2	10.7	391
	578	0.9	90.4	2.9	0.5	6.2	2389
	598	2.1	80.1	15.5	0.9	3.4	4621
740,000	550	0.1	89.3	0.0	3.7	7.0	321
	579	0.8	93.5	0.0	1.0	5.5	2834
	600	1.9	93.3	2.3	0.9	3.4	6458

Feed: 40% N_2/13% O_2/38% CH_4/9% H_2O.

Table 3
Comparison of the performances of V12 with that of the reference samples V/MCM-A and V/MCM-B

Catalyst	V (%)	Feed composition (%) inert/CH_4/O_2/H_2O	GHSV ($L\,kg_{cat}^{-1}\,h^{-1}$)	T (°C)	Conversion (%)	Selectivity (%)				Productivity ($g\,kg_{cat}^{-1}\,h^{-1}$)
						HCHO	CO	CO_2	CH_3OH	
V/MCM-A	2.8	36.6/53.5/9.9/0	180,000	595	3.1	27.6	66.1	5.3	0.6	1091
V12	2.2	40/38/13/9	185,000	581	3.5	74.2	23.1	1.0	1.8	2435
			80,000	585	7.7	48.9	48.2	2.2	0.7	1548
V/MCM-B	3.3	40/38/13/9	80,000	580	5.8	41.9	54.0	3.6	0.5	900

Feed: 40% N_2/13% O_2/38% CH_4/9% H_2O.

Table 4
Best performances reported in the literature for the V/SiO_2 system

Sample	Feed composition (%) inert/CH_4/O_2/H_2O	GHSV ($L\,kg^{-1}\,h^{-1}$)	T (°C)	CH_4 conversion (%)	Selectivity in HCHO (%)	HCHO productivity ($g\,kg_{cat}^{-1}\,h^{-1}$)	Refs.
3.9% V/SBA-15	10/80/10/0	166,000	600	1.8	36.4	1063	[3]
		249,000		1.2	48.2	1370	
		417,000		0.6	63.3	1499	
3% V/SBA-15	37.6/58.3/4.1/0	144,000	625	2.3	95	2490	[11]
	0/95.9/4.1/0			1.6	94	2790	
2.8% V/MCM41	37.0/53.2/9.8/0	180,000	595	3.2	29.1	1083	[4]
		280,000	622	4.7	26.3	2255	
1% V_2O_5/SiO_2	25.8/49.0/6.9/18.3	183,600	625	10.7	4.9	504	[14]
1.6% V_2O_5/SiO_2	20.8/72.0/7.2/0	90,000	580	0.5	75	324	[10]
4.0% V_2O_5/SiO_2				2.6	45	972	

action temperatures. We mention that the V/MCM-A catalyst tested in this study and prepared using the protocol described by Bernt et al. [4] gave catalytic test results similar to those reported previously (Tables 3 and 4).

How adding water to the gas feeds affects V12 performance was investigated in the range 0–30 kPa. Methane conversion increased with increasing water pressure up to 8 kPa and then decreased (Fig. 4A). No strong effect on the selectivity toward formaldehyde was observed, with the exception of that related to the change in conversion. A slight increase in methanol selectivity was noted (Fig. 4B). The optimal HCHO yield was obtained with a water pressure of 8 kPa. These results suggest that water influences mainly the number or accessibility of the active sites and only weakly affects these sites' intrinsic properties. The decreased conversion observed at high water pressures could arise from a preferential adsorption of water on these sites.

The effect of water on V12 catalyst stability was studied by alternatively shifting a charge with 30 kPa of water to a charge without water (Fig. 5). As expected, the activity decreased when water was removed. When the charge was shifted back to the charge containing water, the activity increased but did not reach the initial value; this observation was interpreted as an irreversible change in the number of active sites. However, the decrease in activity was counterbalanced by an increase in selectivity, and the formaldehyde yield regained its initial value.

3.3. Reaction pathway

To determine the reaction pathway, the thermal transformations in the reactor of methanol and a mixture of methanol

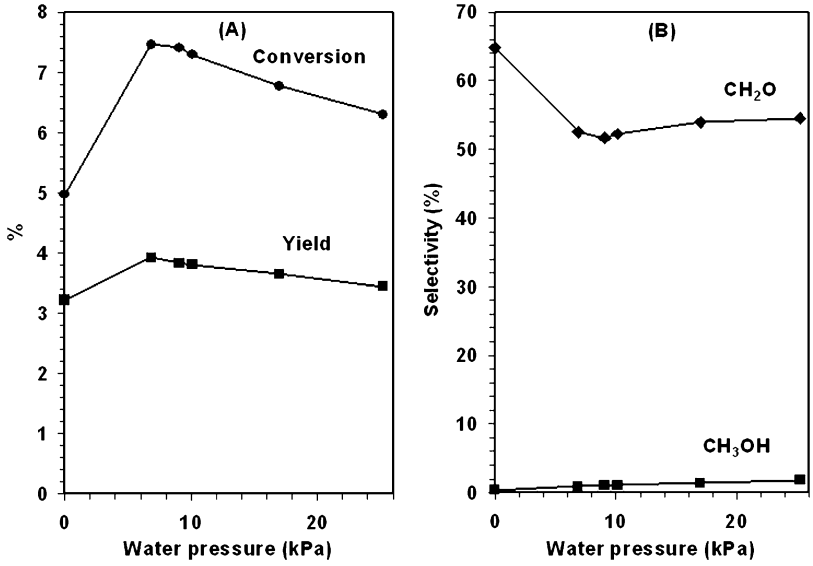

Fig. 4. Influence of addition of water in the feed on: (A) conversion and yield in HCHO, (B) selectivities in HCHO and CH_3OH.

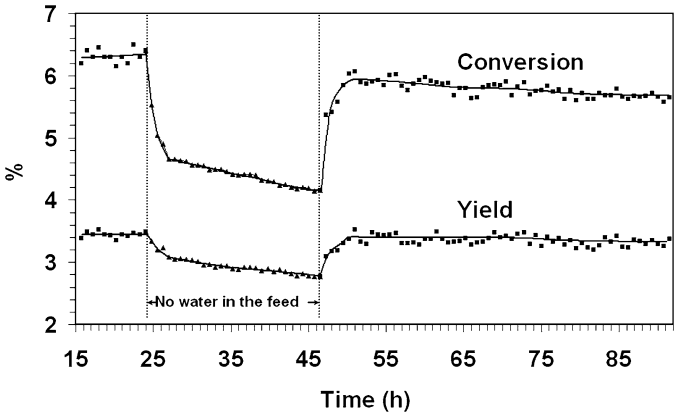

Fig. 5. Effect of removing water in the feed on stability of conversion and yield of the V12 catalyst. 30% of water was alternatively added or not to the gas feed composition.

and formaldehyde were studied at temperatures above 550 °C in the absence of catalyst (Fig. 6). Below 580 °C, methanol transformed to formaldehyde and CO; above 580 °C, only CO_2 was formed (Fig. 6A). Formaldehyde transformed to CO at all temperatures, and CO_2 began to appear in the gas composition above 580 °C (Fig. 6B). This indicated that the increase in CO_2 observed above 580 °C on the catalysts in methane oxidation was related to the degradation of the reaction product.

In the case of methanol conversion, the apparent activation energies of methanol transformation and formaldehyde formation were comparable, whereas that of CO formation was very high. In the case of conversion of the methanol–formaldehyde mixture, the three activation energies were all comparable and close to that of the C–H bond of formaldehyde (360 kJ mol^{-1}). In this latter case, the activation energy for formaldehyde transformation was calculated taking into account the transformation

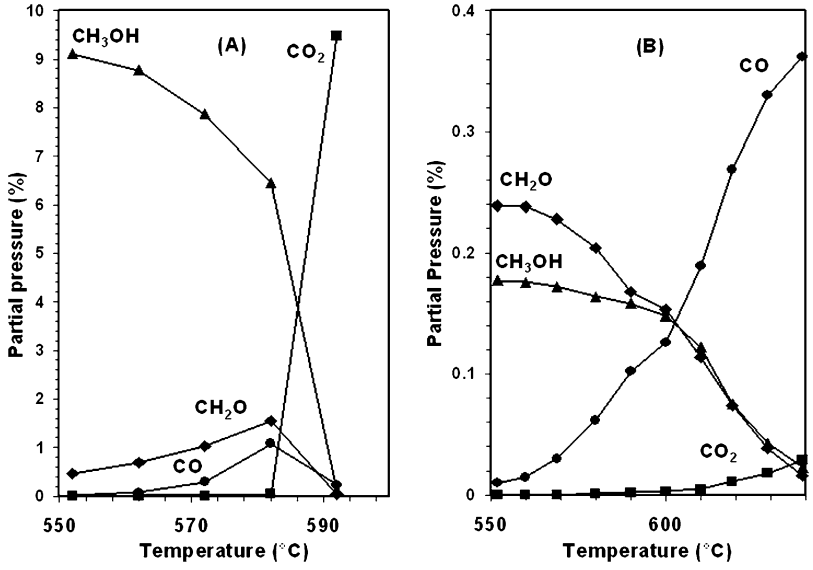

Fig. 6. Evolution of the gas composition during the thermal decomposition of: (A) a mixture 31.97% O_2/58.57% N_2/9.56% CH_3OH and (B) a mixture 35.92% O_2/62.12% N_2/0.25% HCHO/0.18% CH_3OH/1.53% H_2O.

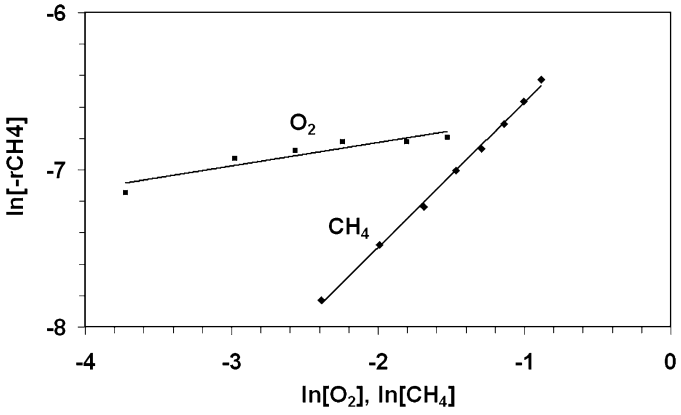

Fig. 7. Arrhenius plot for methane conversion on V12 versus partial pressures of oxygen and methane.

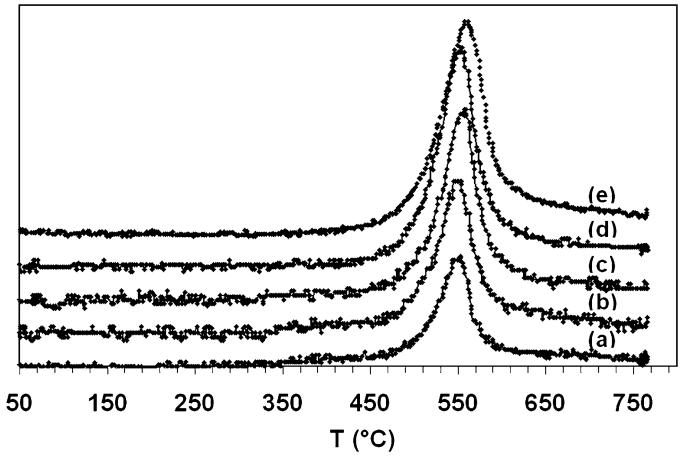

Fig. 8. TPR profiles of: (a) V08, (b) V12, (c) V16, (d) V20 and (e) V24.

of methanol to formaldehyde. Experimentally, the rates considered for the Arrhenius plots corresponded to the formaldehyde consumption, from which the rates of transformation of methanol to formaldehyde had been subtracted. All of the calculated values showed that the main product of methanol degradation was formaldehyde and that of formaldehyde degradation was CO. The main pathways for the thermal transformation of methanol and formaldehyde were thus

$$CH_3OH \rightarrow CH_2O \rightarrow CO \rightarrow CO_2 \quad (1)$$

and

$$CH_2O \rightarrow CO \rightarrow CO_2. \quad (2)$$

Each degradation product could be produced by readsorption or directly in the gas phase. A similar sequence was proposed for partial oxidation of methane, in particular, from TAP experiments: $CH_4 \rightarrow CH_2O \rightarrow CO \rightarrow CO_2$ [27–29]. In this sequence, methane is directly transformed to formaldehyde. Methanol, which could be produced in a parallel manner, was rather unstable, and its selectivity increased with increasing GHSV values.

To calculate the maximal formaldehyde selectivity theoretically achievable if thermal degradation is avoided, the influence of the gas-phase reaction on the degradation of formaldehyde was evaluated. It was observed that the gas-phase contribution was important at the temperature at which the maximum yields were obtained at low flow rates. After checking that no direct thermal transformation of methane occurred in the absence of catalyst, a significant improvement in selectivity was obtained above 580 °C by increasing the gas velocity after the catalytic bed.

The influence of P_{CH_4} and P_{O_2} on the catalytic performance of the solids was investigated, and the activation energy corresponding to the catalytic transformation of methane was calculated (Fig. 7). The reaction order values with respect to oxygen and methane were 0.92 and 0.15, respectively; the reaction may be considered to follow pseudo-first- and zero-order kinetics with respect to methane and oxygen. The activation energy was the same on all of the catalysts ($281 \pm 3\ kJ\,mol^{-1}$). Similar results have been obtained on several other efficient catalysts, including vanadium, molybdenum oxides supported on silica, and pure silica [4,16,28,30–32].

Table 5
Reduction temperature of isolated vanadium species and V dispersion of the catalysts

Sample	Reduction temperature (°C)	Dispersion (%)
V08	547	95
V12	548	90
V16	553	93
V20	550	87
V24	552	82
V/MCM-A	536	65
V/MCM-B	560	72

3.4. Active species characterization

To gain a better understanding of the origin of the high efficiency of the active sites, the catalysts were characterized by TPR measurements and Raman and IR spectroscopies. The TPR curves of the catalysts plotted in Fig. 8 are typical of vanadium-supported compounds with two peaks, one narrow and intense around 550 °C, attributed to isolated species, and the other much smaller and broader at higher temperatures, attributed to polymeric species [3,4,8,33,34]. The dispersion values of vanadium species were calculated by dividing the area of the low-temperature TPR peak by the area of the total TPR profile as proposed in the literature [10,35]. These calculated values and the reduction temperature values of the isolated species are given in Table 5. The dispersion values were much higher than those of V/MCM-A and V/MCM-B, as well as those reported in the literature [10,35]. It can be seen that almost only isolated species were present in the new catalysts up to a vanadium loading of 3 wt%.

The Raman spectra of the compounds recorded in dehydrated conditions at 550 °C in air are presented in Fig. 9. All the spectra showed an intense band at 1037 cm^{-1} attributed to the stretching vibrations of short V=O bonds of isolated distorted vanadium tetrahedra [36–41]. It was proposed from ^{51}V nuclear magnetic resonance results that these species had one short

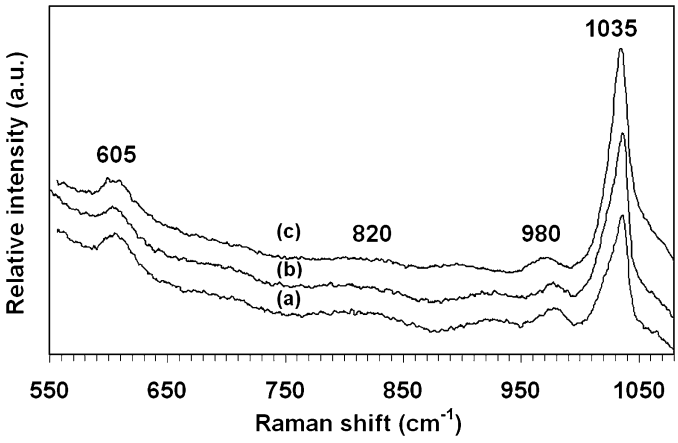

Fig. 9. Raman spectra at 550 °C in air of: (a) V08, (b) V16 and (c) V20.

V=O bond and three long bridging V–O–Si bonds [42,43]. The intensity of this Raman band increased with an increase in V content, whereas no broadening or shift was evidenced. This observation suggested that the number of monomeric species increased and that no additional species were formed. The main band presented a shoulder at 1060 cm^{-1} assigned to perturbed silica vibrations [39,40]. The band near 980 cm^{-1} corresponded to the elongation ν(Si–OH) of silanol groups [36,39,44], and the very broad band around 820 cm^{-1} has been attributed to ν_s(Si–O–Si) vibrations [39,44]. The band at 605 cm^{-1} was due to D2 defect modes, that is, vibrations of cyclic trisiloxane (3-membered rings) species [39,45].

The assignment of the band near 920 cm^{-1} is still ambiguous. It was tentatively attributed to $((VO_3)_n)^{n-}$ polymeric metavanadate chains [36,37]. A detailed study [39] showed that the intensity of this band did not increase significantly with increasing vanadium content. The authors attributed this band and also a band around 1075 cm^{-1} to silica vibrations perturbed by the formation of V–O–Si bonds [39,40]. Interestingly, the band at 920 cm^{-1} was intense when a 10% V_2O_5/SiO_2 compound was partially hydrated [39]. Went et al. [37] suggested that this band could arise from the hydrolysis of Si–O–V bonds on adsorption of H_2O, leading to a hydroxylated vanadium species and silanol groups. Another study also reported that the ν(V=O) vibrations of a vanadium center with one double-bonded oxygen and one hydroxyl group could fall into the 950–1000 cm^{-1} range [36]. Finally, the bands characteristic of crystalline V_2O_5 observed near 995, 700, 520, 404, 305, 258 and 145 cm^{-1} [36–41] and easily detected by micro-Raman spectroscopy were not observed.

Fig. 10 compares the Raman spectra at 550 °C in air of V20 and V/MCM-A, V24, and V/MCM-B, up to 3800 cm^{-1}. For each vanadium content (near 3 and 3.5%), no significant difference was observed in the 600–1200 cm^{-1} frequency range. However, a particular feature was observed concerning the band at 3740 cm^{-1} attributed to ν(SiO–H) stretching vibrations. Indeed, its relative intensity for V20 and V24 was double that for V/MCM-A and V/MCM-B, indicating a higher proportion of silanol groups in the new catalysts. This feature may be common to the V/SBA-15 catalyst, which also exhibited high performances (Table 4).

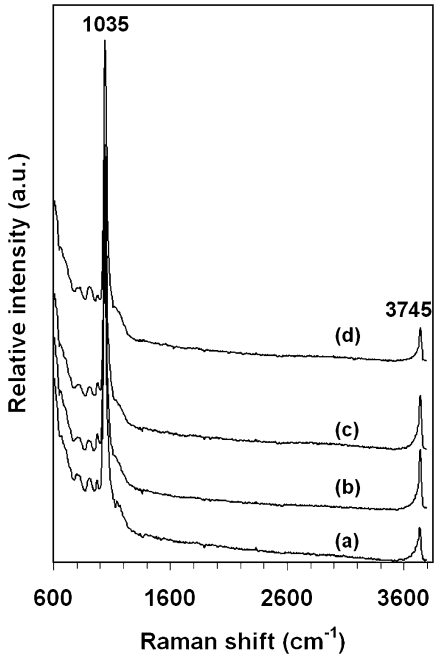

Fig. 10. Comparison of Raman spectra at 550 °C in air of: (a) V/MCM-A, (b) V20, (c) V24 and (d) V/MCM-B.

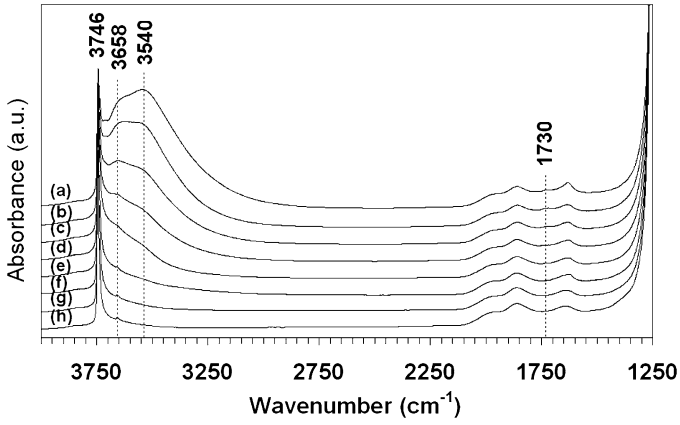

Fig. 11. IR spectra of V12 after treatments in O_2 at: (a) 150 °C, (b) 200 °C, (c) 250 °C, (d) 300 °C, (e) 350 °C, (f) 450 °C, (g) 550 °C and (h) 580 °C.

A pellet of the V12 catalyst was dehydrated in O_2 to characterize the hydroxyl groups by IR spectroscopy. The spectrum recorded after a treatment at 150 °C (Fig. 11a) showed, besides network bands below 2000 cm^{-1}, a strong and narrow band near 3745 cm^{-1} due to ν(O–H) elongation vibrations of isolated terminal silanol groups [4,36,41,46,47] and a large band around 3540 cm^{-1} corresponding to the vibrations of water molecules and hydrogen-bonded SiOH [46]. The intensity of the latter band decreased with increasing temperature and disappeared at 350 °C (Fig. 11e). But the peaks of the terminal silanol groups remained asymmetric up to 580 °C (Fig. 11h), indicating the presence of SiOH interacting with the proton of a nearby hydroxyl group [4,46]. Around 450 °C and above (Figs. 11f–h), an additional band at 3658 cm^{-1} was revealed, attributed to the ν(OH) stretching modes of VO–H bonds [4, 36,41,46–48]. Fig. 12 presents the IR spectra of the V08–V20

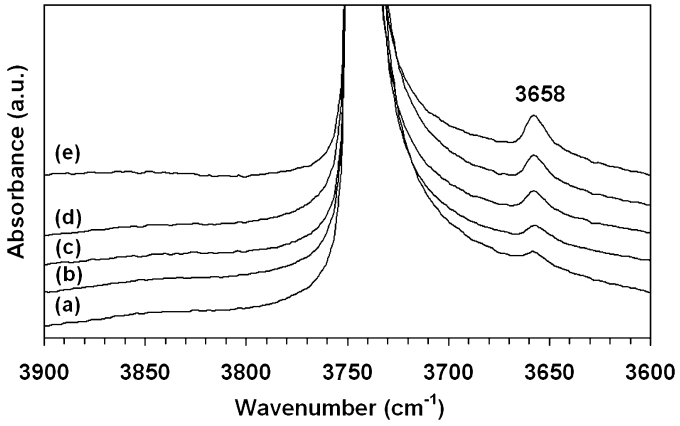

Fig. 12. IR spectra of hydroxyl groups after treatments in O_2 at 580 °C: (a) V08, (b) V12, (c) V16, (d) V20 and (e) V24.

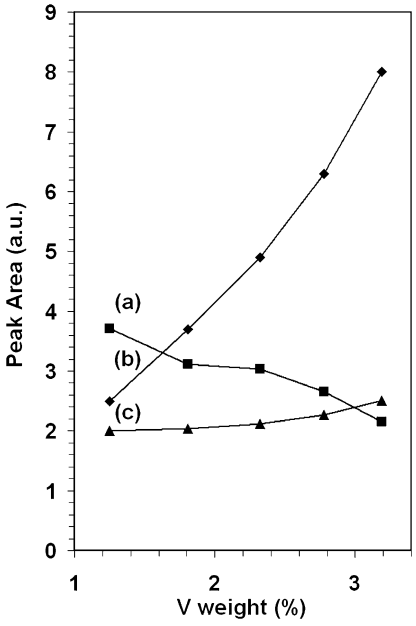

Fig. 13. Evolution with V content of the area of: (a) the ν(SiO–H) peak, (b) the ν(VO–H) peak (×100) and (c) the ν(VO–H) peak normalized relative to the V weight content of the solids (×100).

samples at 3600–3900 cm^{-1} after desorption under dry oxygen at 550 °C for 2 h. The intensities of the bands corresponding to ν(SiO–H) and ν(VO–H)vibrations are plotted in Figs. 13a and b. The intensity of the ν(VO–H) vibrations band is normalized relative to the weight content of the solids in Fig. 13c. As expected, the intensity of the ν(VO–H) vibrations band increased, whereas that of the silanol groups decreased. Extrapolation of the silanol group's vibration intensity to zero led approximately to a theoretical maximum content of supported vanadium species of 6.3%. The normalized peak area of the ν(VO–H) vibrations did not remain constant at high vanadium loading (Fig. 13c). This result could be explained by either the presence of vanadium species without hydroxyl groups (in which case the relative concentration would decrease with increasing vanadium content) or the formation of polymeric species detected by TPR at high vanadium loadings. But it is difficult to consider the second explanation, because in this case each vanadium cation of the additional species should be hydroxylated at least once. The presence of monomeric hydroxylated and nonhydroxylated species in the prepared catalysts is, therefore, the preferred explanation.

4. Discussion

Site isolation is a key aspect in obtaining efficient supported vanadium oxide catalysts. Such isolation can result only from a specific synthesis protocol. Most of the preparation protocols described in the literature involve aqueous impregnations of silica. Silica is a very acidic support, and in acidic aqueous solutions, the stable vanadium species are polynuclear [18–20], which is not favorable to obtaining dispersed supported species. One way to achieve this goal is to use mononuclear precursors during preparation and to try to keep this nuclearity even after calcination and activation.

Five monomeric species can be distinguished in aqueous solutions: VO_2^+, $VO(OH)_3$, $VO_2(OH)_2^-$, $VO_3(OH)^{2-}$, and VO_4^{3-}. Among these species, only $VO(OH)_3$, $VO_2(OH)_2^-$, and $VO_3(OH)^{2-}$ are able to co-condense with $Si(OC_2H_5)_4$ species. $VO(OH)_3$ exists only in a very short pH range, and $VO_3(OH)^{2-}$ can co-condense only via one hydroxyl group. Therefore, the best vanadium precursor for co-condensation with the silicon alkoxide species was $VO_2(OH)_2^-$. The pH and concentration of the starting solution was thus chosen to stabilize these species preferentially. The preparation procedure described in this paper optimized the pH and concentration parameters, leading to the stabilization of this species and the conditions of its co-polymerization with the silicon ones.

The synthesized solids were characterized by a high surface area, typical of mesoporous compounds, with vanadium species well dispersed at the surface (Tables 1 and 5). However, this dispersion decreased slightly with increasing vanadium content, as well as the surface area.

The catalytic properties in the oxidation of methane to formaldehyde were determined and compared with those of catalysts of the same type prepared as described previously. This comparison was conducted not only in terms of conversion selectivity, but also in terms of productivity. In both cases, the new catalysts appeared to be the most efficient ones (Tables 2–4). In parallel, the study of different reaction parameters, such as oxygen and methane partial pressures and reaction temperature, showed that the same type of mechanism was involved in formaldehyde and methanol formation. The origin of the high efficiency of the catalysts had to be searched for in the nature of the catalytic sites.

The best selectivities were obtained with the most highly dispersed samples (Fig. 2; Table 5). The compounds with higher vanadium content were more active but less selective. The monomeric species were then confirmed to be the most selective species.

Site isolation is certainly necessary to avoid the consecutive oxidation of the formaldehyde formed and to obtain high selectivity in that product. The activity in methane oxidation increased with an increasing amount of vanadium active species. However, site isolation is difficult to obtain along with high

vanadium content. The dispersions previously reported from TPR measurements on V/SiO_2 catalysts were rapidly limited, because oligomeric or bulk-like V_2O_5 were formed even at low vanadium contents [3,4,6,10,12]. Our new catalysts exhibited a higher dispersion of vanadium species, as shown by TPR measurements (Table 5). The dispersion was >90% up to a vanadium content of 2.5 wt%.

The characterization of the compound showed that at least two monomeric species should be distinguished. These species correspond to a vanadium cation with one V=O bond and three bridging V–O–Si bonds, or two bridging V–O–Si bonds and one hydroxyl group. The V=O bond is characterized by its stretching vibration near 1035 cm^{-1}, and the VO–H bond is characterized by its stretching vibration near 3658 cm^{-1}. Such species, which were shown to be stable at 600 °C both in air and in the feed, are presently under study by other characterization techniques.

The presence of hydroxylated vanadium species has been reported previously [4,36,46–48]. However, no quantitative comparison is possible, because the molar extinction coefficient of the 3658 cm^{-1} band is unknown. Interestingly, significant increases of the band at 3660 cm^{-1} were reported after treatment with steam at 600 °C [4] or adsorption of a small quantity of water at room temperature [36]. These enhancements pointed out the formation of additional V–OH groups by hydrolysis of V–O–Si bridging bonds.

It was observed that the mesoporous silica as synthesized exhibited a high concentration of silanol groups characterized on IR and Raman spectroscopy by their stretching vibrations near 3740 cm^{-1}. Vicinal SiOH groups required to anchor vanadium species could be provided by hydrolyzed three-membered rings of silica [39].

Silanol groups may be involved in the oxido-reduction mechanism of the proposed active site, allowing the stabilization of a vanadium oxide center (V^{4+}–O^-) capable of H abstraction from methane. The study of the complete oxido–reduction process of the monomeric vanadium species has been undertaken. Finally, the beneficial effect on formaldehyde yield of adding water may be related in part to a high level of hydroxylation of the catalysts.

5. Conclusion

A new method of preparation of vanadium-supported based catalysts has been described. It led to the most productive known catalysts of this type for methane oxidation to formaldehyde. This higher space–time yield is related to both a higher activity and a higher selectivity toward formaldehyde. The higher activity results from a higher quantity of the most active species, the monomeric vanadium species. The higher selectivity may be attributed to the high dispersion of the vanadium, because isolated monomeric species appear to be more selective than the others, as well as to a higher concentration of isolated species. These species contain one V=O bond and three bridging V–O–Si bonds or one hydroxyl group and two bridging V–O–Si bonds. The active and selective catalysts are also characterized by a higher concentration of silanol groups at their surface. This latter species may take part directly in the redox reaction mechanism, facilitating regeneration of the active and selective sites, or in the activation of methane.

Although the intrinsic properties of the catalysts appear to be crucial to obtaining selective catalysts, the degradation of formaldehyde in the catalytic test conditions is an important parameter as well. Using low contact times and adding water to the gas feed allowed to significantly reduce this degradation and to optimize catalyst productivity.

Acknowledgments

The authors are grateful to the Région Rhône-Alpes for initiating this research and partially financing it as part of an Emergence Program.

References

[1] R.G. Herman, Q. Sun, C. Shi, K. Klier, C.-B. Wang, H. Hu, I.E. Wachs, M.M. Bhasin, Catal. Today 37 (1997) 1.
[2] K. Otsuka, Y. Wang, Appl. Catal. A 222 (2001) 145.
[3] V. Fornes, C. Lopez, H.H. Lopez, A. Martinez, Appl. Catal. A: Gen. 249 (2003) 345.
[4] H. Berndt, A. Martin, A. Brückner, E. Schreier, D. Mûller, H. Kosslick, G.U. Wolf, B. Lücke, J. Catal. 191 (2000) 384.
[5] T. Sugino, A. Kido, N. Azuma, A. Ueno, Y. Udagawa, J. Catal. 190 (2000) 118.
[6] A. Kido, H. Iwamoto, N. Azuma, A. Ueno, Catal. Surv. Japan. 6 (1/2) (2002) 45.
[7] A. Ueno, N. Azuma, K. Aoki, T. Sugino, European Patent 1038578 (2000).
[8] F. Arena, N. Giordano, A. Parmaliana, J. Catal. 167 (1997) 66.
[9] M.J. Koranne, J.G. Goodwin Jr., G. Marcellin, J. Phys. Chem. 97 (1993) 673.
[10] M.M. Koranne, J.G. Goodwin Jr., G. Marcelin, J. Catal. 148 (1994) 388.
[11] B. Lin, X. Wang, Q. Guo, W. Yang, Q. Zhang, Y. Wang, Chem. Lett. 32 (9) (2003) 860.
[12] Q. Zhang, Y. Wang, Y. Ohishi, T. Shishido, K. Takehira, J. Catal. 202 (2001) 308.
[13] V. Luca, D.J. MacLachlan, K. Morgan, Chem. Mater. 9 (1997) 2720.
[14] C.-B. Wang, R.G. Herman, C. Shi, Q. Sun, J.E. Roberts, Appl. Catal. A: Gen. 247 (2003) 321.
[15] M. Morey, A. Davidson, H. Eckert, G. Stucky, Chem. Mater. 8 (1996) 486.
[16] N.D. Spencer, C.J. Pereira, J. Catal. 116 (1989) 399.
[17] L. N'Guyen, J.M.M. Millet, S. Loridant, French patent 03.07269 (2003).
[18] B.M. Weckhuysen, D.E. Keller, Catal. Today 2811 (2001) 1.
[19] C.F. Base, R.E. Mesmer, The Hydrolysis of Cation, Wiley, New York, 1970.
[20] D.L. Kepert, The Early Transition Elements, Academic Press, London, 1972.
[21] D. Kumar, K. Schumacher, C. du Fresne von Hohenesche, M. Grün, K.K. Unger, Colloids Surf. Physicochem. Eng. Aspects 187–188 (2001) 109.
[22] E.P. Barett, L.G. Joyner, P.P. Halende, J. Am. Chem. Soc. 73 (1951) 373.
[23] B.C. Lippens, J.H. de Boer, J. Catal. 4 (1965) 319.
[24] B.C. Lippens, B.G. Linsen, J.H. de Boer, J. Catal. 3 (1964) 32.
[25] P.T. Tanev, M. Chibwe, T.J. Pinnavaia, Nature 368 (1994) 317.
[26] J. March, Advanced Organic Chemistry, third ed., Wiley, New York, 1985.
[27] B. Kartheuser, B.K. Hodnett, H. Zanthoff, M. Baerns, Catal. Lett. 21 (1993) 209.
[28] A.W. Sexton, B.K. Hodnett, in: R.K. Grasselli, S.T. Oyama, A.M. Gaffney, J.E. Lyons (Eds.), 3rd World Congress on Oxidation Catalysis, Elsevier, 1997, p. 1129.
[29] B. Kartheuser, B.K. Hodnett, H. Zanthoff, M. Baerns, in: M.M. Bhasin, D.W. Slocum (Eds.), Methane and Alkane Conversion Chemistry, Plenum Press, New York, 1995, p. 195.

[30] R.L. McCormick, M.B. Al-Sahali, G.O. Alptekin, Appl. Catal. A: Gen. 226 (2002) 129.
[31] F. Arena, A. Parmalianna, Acc. Chem. Res. 36 (12) (2003) 867.
[32] L. Zhong, F.-L. Qiu, M.-Y. Zhao, J. Nat. Gas Chem. 4 (1992) 363.
[33] V. Sokolovskii, F. Arena, S. Coluccia, A. Parmaliana, J. Catal. 173 (1998) 238.
[34] Y.-M. Liu, Y. Cao, N. Yi, W.-L. Feng, W.-L. Dai, S.-R. Yan, H.-Y. He, K.-N. Fan, J. Catal. 224 (2004) 417.
[35] M.M. Koranne, J.G. Goodwin Jr., G. Marcelin, J. Catal. 148 (1994) 369.
[36] M. Schraml-Marth, A. Wokaun, M. Pohl, H.-L. Krauss, J. Chem. Soc. Faraday Trans. 87 (16) (1991) 2635.
[37] G.T. Went, S.T. Oyama, A.T. Bell, J. Phys. Chem. 94 (1990) 4240.
[38] S.T. Oyama, G.T. Went, K.B. Lewis, A.T. Bell, G.A. Somorjai, J. Phys. Chem. 93 (1989) 6786.
[39] X. Gao, S.R. Bare, B.M. Weckhuysen, I.E. Wachs, J. Phys. Chem. B 102 (1998) 10842.
[40] X. Gao, S.R. Bare, J.L.G. Fierro, I.E. Wachs, J. Phys. Chem. B 103 (1999) 618.
[41] M. Baltes, K. Cassiers, P. Van Der Voort, B.M. Weckhuysen, R.A. Schoonheydt, E.F. Vansant, J. Catal. 197 (2001) 160.
[42] H. Eckert, I.E. Wachs, Mater. Res. Soc. Symp. Proc. 111 (1988) 459.
[43] H. Eckert, I.E. Wachs, J. Phys. Chem. 93 (1989) 6796.
[44] Q. Sun, J.M. Jehng, H. Hu, R.G. Herman, I.E. Wachs, K. Klier, J. Catal. 165 (1997) 91.
[45] C.J. Brinker, R.J. Kirkpatrick, D.R. Tallant, B.C. Bunker, B. Montez, J. Non-Cryst. Solids 99 (1988) 418.
[46] S. Dzwigaj, El M. El Malki, M.-J. Peltre, P. Massiani, A. Davidson, M. Che, Top. Catal. 11/12 (2000) 379.
[47] G. Martra, F. Arena, S. Coluccia, F. Frusteri, A. Parmaliana, Catal. Today 63 (2000) 197.
[48] P. Van der Voort, M.G. White, M.B. Mitchell, A.A. Verberckmoes, E.F. Vansant, Spectrochim. Acta, Part A 53 (1997) 2181.